Crossover behavior of critical helix fluctuations in MnSi

S. V. Grigoriev,[1,*] S. V. Maleyev,[1] E. V. Moskvin,[1] V. A. Dyadkin,[1] P. Fouquet,[2] and H. Eckerlebe[3]
[1]*Petersburg Nuclear Physics Institute, Gatchina, 188350 St. Petersburg, Russia*
[2]*Institut Laue-Langevin, BP 156, 38042 Grenoble Cedex 9, France*
[3]*GKSS Forschungszentrum, 21502 Geesthacht, Germany*
(Received 4 December 2009; revised manuscript received 3 February 2010; published 12 April 2010)

The critical helix fluctuations in the cubic noncentrosymmetric helimagnet MnSi have been studied by means of neutron small angle scattering and spin echo spectroscopy. To interpret the data, analytical formulas for the susceptibility in real space were obtained for the first time. The calculations presented here are based on the theory introduced in S. V. Grigoriev *et al.*, Phys. Rev. B **72**, 134420 (2005). According to this theory the temperature in the critical region can be divided into three parts with different types of chiral fluctuations: (i) ferromagnetic like; (ii) isotropic helical; and (iii) anisotropic helical ones. The fluctuations increase in amplitude with a randomly oriented but left-skewed pitch **k** upon approaching T_c=29 K. The scaling law of the inverse correlation length κ exhibits a crossover at $\kappa \approx k$. The value of the critical exponent ν is changed from ν_1=0.40(6) in the vicinity of T_c to ν_2=0.68(1) at high temperatures. The critical behavior of the relaxation rate Γ along the easy direction obeys the dynamical scaling $\Gamma \sim \kappa^Z \sim \tau^{Z\nu}$ with a crossover at the temperature where $\kappa \approx k$ with Z_1=2.5(1) for the high temperatures and Z_2=1.10(3) close to T_c. Fluctuations become 100% left handed at the crossover point. The observed crossover is associated with the dominating influence of the Dzyaloshinskii-Moria interaction near T_c, responsible for the chiral ordering.

DOI: 10.1103/PhysRevB.81.144413 PACS number(s): 61.05.fg, 75.40.−s, 75.50.Cc, 76.60.Lz

I. INTRODUCTION

The increasing number of publications devoted to the magnetic and transport properties of cubic magnets with the space group $P2_13$ such as MnSi and related compounds FeGe, $Fe_{1-x}Co_xSi$ is evidence of the importance of problems related to this system: (i) the quantum phase transition under applied pressure[1–4] and (ii) a puzzle of the left-handed chirality of the spin helix.[5–8] None of these problems is really solved up to now, but even the magnetic phase transition at ambient pressure is still a subject of debates.[9–14] The complex critical behavior is a result of the hierarchy of interactions in this system (Bak-Jensen model).[15] Strong ferromagnetic exchange (FE) is responsible for long-range magnetic order. As it is well established, the antisymmetric Dzyaloshinskii-Moriya interaction (DMI) caused by the lack of the center of symmetry in Mn atomic arrangement gives rise the spiral spin structure of this cubic magnets.[15,16] The DMI is isotropic itself due to the cubic symmetry, so the helix vector **k** of the magnetic spiral in MnSi is fixed along one of the cube diagonals by the weak anisotropic exchange interaction (AEI).[15]

The magnetic phase transition in this compound has been identified as a first order in a very narrow temperature range $T_c \pm 0.1$ K. On the other hand, it is also recognized that the first-order feature at T_c is just a minor part of the critical behavior above T_c, which is marked by the rounded maxima or minima of heat capacity, thermal expansion coefficient, sound velocities and absorption, and the temperature derivative of resistivity.[12,13]

It was shown recently that the critical region above T_c has two distinct parts: a pure chiral fluctuating part, which is observable over a temperature range of one kelvin in the vicinity of T_c and the paramagnetic partially chiral part at higher temperatures.[14] It was suggested that the first part was a candidate for the spontaneous fluctuating skyrmion phase,[14] which was assumed in Ref. 17. Although based on the modified Bak-Jensen hierarchy of the interactions, the skyrmionic picture has a cylinderlike one-dimensional symmetry with the wave vector **k** perpendicular to the symmetry axis. This spin texture obviously differs from the widely accepted helix-like spin texture that has a planelike two-dimensional (2D) symmetry with the wave vector **k** perpendicular to the plane. This helix fluctuating picture had been applied in[10,11] and it is used in this paper to interpret the polarized SANS measurements conducted for the spin fluctuations in MnSi.

In the following sections, we demonstrate in more detail than in our earlier works[10,11] that existing experimental data are in good qualitative agreement with conventional mean-field results presented in Ref. 10 which catches principal symmetry features of the problem. It was shown in Ref. 10 that the randomly oriented left-handed chiral spin fluctuations persist above T_c. Due to AEI these fluctuations increase strongly along the easy directions ⟨111⟩ only and are suppressed in other directions. The correlation length of fluctuations along ⟨111⟩ obeys the scaling law with the corresponding critical exponent equals to ν=0.62(1). In the subsequent paper[11] the critical exponent of the correlation length has been determined over a wider temperature range than in Ref. 10 (two decades on τ scale) and the obtained value is given by ν=0.68(3). According to both papers[10,11] (see also Sec. II) the AEI plays a significant role around the easy directions only and detailed study of the critical fluctuations in this region can clarify the real nature of the phase transition, which apparently cannot be done by macroscopic measurements. Indeed, in case of macroscopic or poorly resolved neutron-scattering measurements the critical fluctuations from the whole momentum space contributes to the measured quantities and therefore smears out anisotropic features of the problem.

We have revised the data from the previous paper[11] and present the additionally collected ones. The combined set of the scans in the easy direction taken from two different samples shows that the scaling law for the inverse correlation length undergoes a crossover at $\kappa \approx k$. The critical exponent close to T_c is $\nu_1=0.40(6)$ and changes to $\nu_2=0.68(1)$ at high temperatures. The susceptibility at $\mathbf{Q}\|\mathbf{k}$ displays a similar crossover. This crossover is a transition to the pure chiral fluctuating phase near T_c reported in.[14] Using neutron spin echo (NSE) measurements we study the critical dynamic of MnSi along the easy direction. It is shown that the relaxation rate of the critical fluctuations Γ measured at $|\mathbf{q}|=|\mathbf{Q}-\mathbf{k}|$ reveals a behavior that is compatible with the dynamic scaling assumptions. The scaling law at $q<\kappa$ obeys $\Gamma \sim \kappa^Z \sim \tau^{Z\nu}$ and undergoes a crossover at the same temperature as for the above-mentioned static data, with $Z_1=2.5(1)$ for the high τ and $Z_2=1.10(4)$ close to T_c. For $q>\kappa \gtrsim k$ we found $\Gamma \sim q^{5/2}$ as in ferromagnets in agreement with the predicted crossover.

Thus, we demonstrate that the magnetic phase transition in MnSi displays two crossovers and three different regimes of the critical fluctuations in agreement with the hierarchy of the interactions in the Bak-Jensen model. First, one observes the ferromagnetic such as fluctuations at high T, which are well distributed over the whole $\mathbf{Q}$ space. Then—with decreasing T—the DMI localizes them in the spherical layer with radius $\mathbf{Q}=k$ and thickness κ. At even lower temperatures T, the layer thickness decreases along the easy directions, while in all other directions it remains finite.

Moreover, our theoretical picture based on the helix fluctuation mean-field theory explains the origin of this crossover into the purely chiral critical region. Therefore, we do not see any feature of experimental data which would disagree with this approach and demand the skirmion assumption. The above-mentioned assumption is based on observation that chiral part of the scattering just above T_c was not described by Eq. (4) in Ref. 14 which was derived in the mean-field approximation.[10] It is not surprising as soon as this approximation cannot give quantitative predictions in the very vicinity of the transition temperature. Yet, the deviation of the experimental data from the predictions of the MF theory does not exceed 10%. At the same time the skyrmion theory, at least in its present form, does not give any predictions on the susceptibility or neutron cross section,[17] which could be verified experimentally. Hence we cannot share the belief to the observation of the skirmionic fluctuating state. It was also claimed in[18] that the long-range skirmionic order was observed in narrow range of the magnetic field below T_c (A phase). We do not think that there is any connection of this reported high-field phase below T_c with the zero-field critical fluctuations above T_c.

The outline of this paper is the following: the essence of the theory for the critical spin fluctuations in MnSi and related compounds is given in Sec. II. The results of the polarized SANS experiments demonstrating the crossover in the inverse correlation length, susceptibility and chirality behavior are presented in Sec. III. In Sec. IV we show the results of the paramagnetic NSE experiment, which gives the time relaxation of the critical fluctuations in the same temperature range. Sec. V presents the discussion and the concluding remarks.

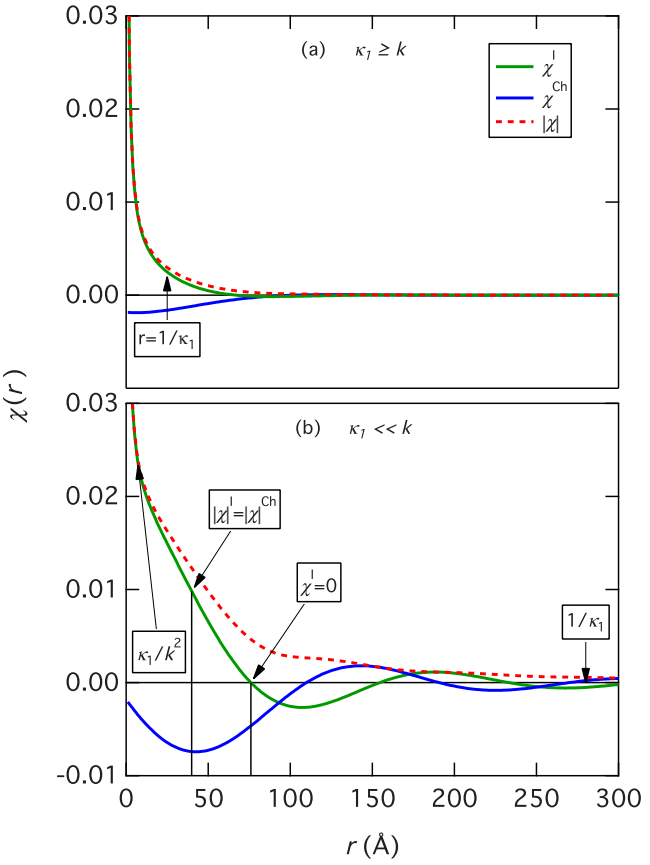

FIG. 1. (Color online) Isotropic, χ^I, and chiral, χ^{Ch}, parts of susceptibility (6) and the sum, $|\chi|=\sqrt{(\chi^I)^2+(\chi^{Ch})^2}$, for two limiting cases: (a) $\kappa_1 \geq k$ and (b) $\kappa_1 \ll k$.

II. THEORETICAL BACKGROUND

For a better understanding and interpretation of the experimental data presented below we outline here the principal theoretical results obtained in Ref. 10 and explain the physical origin of the observed crossovers. A theoretical description of the helical fluctuations within the paramagnetic phase starts with the bilinear part of the free-energy density which is given by[15]

$$W(\mathbf{Q}) = \left[\frac{B}{2}(Q^2+\kappa_0^2)\delta_{\alpha\beta} + iD\epsilon_{\alpha\beta\gamma}Q_\gamma\right] S^\alpha_{\mathbf{Q}} S^\beta_{-\mathbf{Q}} + \frac{F}{2}(Q_x^2|S^x_{\mathbf{Q}}|^2 + Q_y^2|S^y_{\mathbf{Q}}|^2 + Q_z^2|S^z_{\mathbf{Q}}|^2), \quad (1)$$

where the first, second, and third term correspond to the isotropic exchange, the DMI, and the AEI, respectively. The exchange constant B is the spin-wave stiffness at $T=0$ (notified as A in Ref. 19) and we assume $B \gg Da \gg F$, where a is the lattice spacing. Neglecting DMI and AEI terms we get a conventional mean-field expression for the ferromagnetic free-energy. The corresponding susceptibility, $\chi^F(\mathbf{Q})$, is given by well known expression

$$\chi^F_{\alpha\beta}(\mathbf{Q}) = \frac{T}{B(Q^2+\kappa_0^2)}\delta_{\alpha\beta}, \tag{2}$$

where $\kappa_0^2=(C/a^2)(T-T_{c_0})$, $C\sim 1/T_{c_0}$, and T_{c_0} is the ferromagnetic transition temperature.

In the real space we have

$$\chi^F_{\alpha\beta}(\mathbf{r}) = \frac{1}{(2\pi)^3}\int \chi^F_{\alpha\beta}(\mathbf{Q})e^{-i\mathbf{Qr}}d^3\mathbf{Q} = \frac{T}{4\pi B}\frac{e^{-\kappa_0 r}}{r}\delta_{\alpha\beta}, \tag{3}$$

and parameter κ_0 can be interpreted as the inverse correlation length of the ferromagnetic fluctuations.

As was shown in Ref. 10 the second and third terms in Eq. (1) lead to the more complex expression for the susceptibility

$$\chi_{\alpha\beta}(\mathbf{Q}) = \frac{T[(Q^2+k^2+\kappa_1^2)\delta_{\alpha\beta} - 2ik(D/|D|)\epsilon_{\alpha\beta\gamma}Q_\gamma - 4k^2Q_\alpha Q_\beta/(Q^2+k^2+\kappa_1^2)]}{B\{[(Q+k)^2+\kappa_1^2][(Q-k)^2+\kappa_1^2] - 4(F/B)k^2Q^4\{\hat{Q}^4\}/(Q^2+k^2+\kappa_1^2)\}}, \tag{4}$$

where higher-order terms of (F/B) were omitted, $k=|D|/B$ is the helix wave vector at $T<T_c$,[15,19] $\kappa_1^2=\kappa_0^2-k^2=(C/a^2)(T-T_{c_1})$. The parameter κ_1 is a renormalized inverse correlation length, which interpretation is not trivial since it has to be compared to another natural scaling parameter $k=2\pi/d$. The transition temperature T_{c_1} is also renormalized by DMI and it appears that presence of DMI increases the ordering temperature

$$T_{c_1} = T_{c_0} + \frac{k^2a^2}{C}. \tag{5}$$

In the last term of the denominator $\{\hat{Q}^4\}=(Q_x^4+Q_y^4+Q_z^4)/Q^4$ is a cubic invariant. It describes the effect of AEI and links the critical fluctuations to the cubic principal axes. The susceptibility $\chi_{\alpha\beta}$ consists of three parts: the first term in Eq. (4) describes isotropic spin fluctuations as in ferromagnets above T_c. The second term stems from the chiral fluctuations driven by isotropic DMI and the last term gives longitudinal fluctuations along the momentum $\mathbf{Q}$. The first two parts were used in Refs. 10 and 11 for an explanation of the polarized SANS experiments. The last longitudinal term $\chi^L(\mathbf{Q})$ is important for neutron magnetic scattering close to the nuclear Bragg reflections.

The corresponding expression for the small-angle polarized-neutron cross section is given by

$$\frac{d\sigma}{d\Omega} = \frac{2r^2T}{B}\frac{Q^2+k^2+\kappa_1^2+2k(D/|D|)(\mathbf{Q}\cdot\mathbf{P}_0)}{[(Q+k)^2+\kappa_1^2][(Q-k)^2+\kappa_1^2]+k^2\kappa_A^2(\mathbf{Q})}, \tag{6}$$

where $r=5.410^{-13}$ cm and

$$\kappa_A^2(\mathbf{Q}) = -\frac{4FQ^4\{\hat{Q}^4\}}{B(Q^2+k^2+\kappa_1^2)}. \tag{7}$$

In MnSi the κ_A term determines the scattering behavior in small regions around the cubic diagonals only (see below).[10]

Neglecting the last term in the denominator we get critical fluctuations that are maximal at the sphere $Q=k$ with the width $\kappa_1\sim T-T_{c_1}$ in contradiction to the conventional critical behavior, where fluctuations are maximal at the point corresponding to the wave vector of the magnetic structure below T_c. This unusual shape of the scattering intensity was observed in Refs. 3, 10, and 11. However, if $\kappa_1\gg k$ one can neglect k in Eq. (4) and $\chi(\mathbf{Q})$ acquires the conventional ferromagnetic form [Eq. (2)] with $\kappa_0\to\kappa_1$ and weak corrections. This crossover can be seen easily in real space since it occurs due to competition of two scales: inverse correlation length $1/\kappa_1$ and the helix pitch $2\pi/k$ as well as nontrivial symmetry of the fluctuations. To illustrate this point it is instructive to consider the susceptibility in real space, where instead of Eq. (3), we get the following expressions for the isotropic, the chiral, and the longitudinal parts of the susceptibility

$$\chi^I_{\alpha\beta}(r) = \frac{T}{4\pi B}\frac{e^{-\kappa_1 r}}{r}\left(\cos kr + \frac{k}{\kappa_1}\sin kr\right)\delta_{\alpha\beta},$$

$$\chi^{Ch}_{\alpha\beta}(r) = \frac{T}{4\pi B}(D/|D|)\frac{e^{-\kappa_1 r}}{r}\left[\sin kr + \frac{k}{\kappa_1}\left(\frac{\sin kr}{kr} - \cos kr\right)\right]\epsilon_{\alpha\beta\gamma}\hat{r}_\gamma,$$

$$\chi^L_{\alpha\beta}(r) = \frac{T}{4\pi B(k^2+\kappa_1^2)}\nabla_\alpha\nabla_\beta\frac{1}{r}\left[e^{-\kappa_1 r}\left(\frac{k}{\kappa_1}\sin kr - \cos kr\right) + e^{-r\sqrt{k^2+\kappa_1^2}}\right], \tag{8}$$

where $\hat{r}_\gamma=r_\gamma/r$.

When $r\to 0$, the isotropic part displays a $1/r$ singularity, while the other parts remain finite [for instance $|\chi^{Ch}|=Tk/(4\pi B)$]. The expressions in Eq. (8) should be considered in two limiting cases: (i) $\kappa_1\gg k$ realized at high temperatures and (ii) $\kappa_1<k$ close to T_{c_1}. The isotropic and chiral susceptibilities for these two cases are sketched on Fig. 1. To plot the chiral susceptibility we used a negative value for the Dzyaloshinskii constant, D, as it is well established for MnSi.[20,21] In case (i) due to the exponential factor $\exp(-\kappa_1 r)$, which decreases rapidly when $\kappa_1 r$ is larger than one,

we have $kr \ll 1$ and the isotropic part of the susceptibility has the form given by Eq. (3) with replacing $\kappa \to \kappa_1$ and with only a small correction proportional to $\exp(-\kappa_1 r)k^2/\kappa_1$. The other parts of the susceptibility, χ^{Ch} and χ^L, are small. For example, we find $\chi^{Ch} \sim k \exp^{-\kappa_1 r}$. Hence, we have ferromagnetic type of fluctuations. It is well seen in Fig. 1(a), that the isotropic correlations dominate over the chiral for $r \lesssim 1/\kappa_1$, while they all are strongly dumped for $r \gg 1/\kappa_1$. The chiral susceptibility, χ^{Ch}, has no extrema at $r \lesssim 1/\kappa_1$ and is minimal at $r=0$. This leads to the situation, when the left twist of the helix fluctuations have a weak diffuse character: they are all left handed, but with poorly defined helix period.

The crossover occurs around $\kappa_1 \sim k$ and the critical regime fully develops for $\kappa_1 \ll k$ [see Fig. 1(b)]. In this case for the very short distances $r \ll \kappa_1/k^2$ the isotropic part χ^I dominates over χ^{Ch} and χ^L due to the $1/r$ singularity, while for the larger r, $\kappa_1/k^2 \ll r \ll 1/\kappa_1$, the k/κ_1 terms in Eq. (8) become significant and the chiral and longitudinal parts of the susceptibility are of the order of χ^I.

There are two important points on the r scale: (i) when the amplitudes of χ^I and χ^{Ch} are equal, which fixes the value $kr \approx \pi/2$ and (ii) when $\chi^I=0$ corresponding to the value $kr \approx \pi$ [see Fig. 1(b)]. The first point corresponds to the situation, when the modulus of the chiral susceptibility, $|\chi^{Ch}|$, has a maximum at a certain r. The $\pi/2$ twist of the helix fluctuations gets locked-in on the distance of a quarter of the helix period $r=d/4$. This lock-in of the twist for all $\kappa < 2k/\pi$ has two important consequences such as the well established maximum in scattering at $Q=k$ (the ring of scattering) and simultaneously purely chiral fluctuations. Both facts are caused by the minimum in $|\chi^{Ch}(r)|$ at $r \approx d/4$. They have been observed for the first time in Ref. 10 and they were misinterpreted in Refs. 14 and 17 as a signature of a skyrmion phase in contrast to the present interpretation.

The second r point is associated with transformation of the moduli $|\chi|$ from the "high" susceptibility region with $kr \approx \pi/2$ and $\chi^I \sim \chi^{Ch} \approx T/(4B)k^2/\kappa_1$ to the "low" susceptibility region with $kr=\pi n$ where n is integer and $\chi^I \sim \chi^{Ch} \approx T/(4B)k^2/\kappa_1(1/\pi n)$. The physical interpretation of the second point is the following: the probability of fluctuations with $r < k/\pi$ is much higher than of those with $r > k/\pi$. Therefore, the number of "short" wave fluctuations is bigger than the number of "long" wave ones and the average correlation length on approaching T_c from high T has to saturate around the value of $r=\pi/k$.

In the consideration above we have neglected the AEI, although anisotropy is taken into account and the F term in the denominator in Eq. (4) determines the easy directions. According to Ref. 15 the invariant $\{\hat{Q}^4\}$ has two extrema equal to 1 and 1/3 for $\mathbf{Q}$ along the $\langle 100 \rangle$ and $\langle 111 \rangle$ directions, respectively. As a result, the cubic edge and diagonal are the easy directions for positive and negative F, respectively. In the case of MnSi we have $F<0$ and the denominator at $(Q-k) \ll k$ and $\kappa_1 \ll k$ is given by[10]

$$Z = 4Bk^2[(Q-k)^2 + \kappa^2 + (|F|k^2/2B)(\{\hat{Q}^4\} - 1/3)], \quad (9)$$

where $\kappa^2 = \kappa_1^2 + |F|k^2/6B = (C/a^2)(T-T_c)$ and $T_c = T_{c_1} - |F|(ka)^2/(6BC) < T_{c_1}$ is the mean-field transition temperature. Near the minimum we have $\{\hat{Q}^4\} - 1/3 \simeq 8\Phi^2/9 + 3\Theta^2/2$, where Φ and Θ are spherical angles in the frame with z axis along the cubic diagonal.[22] Hence at $(Q-k)^2 \lesssim (|F|k^2/B)$ and $\Theta, \Phi \ll 1$ we have $3D$ critical fluctuations peaked along cubic diagonals. Thus, the AEI restores conventional behavior of the critical fluctuations in the very vicinity of the transition. It follows from Eq. (9) that the correlation length

$$\xi(\mathbf{Q}) = [\kappa^2 + (|F|k^2/2B)(\{\hat{Q}^4\} - 1/3)]^{-1/2} = [\kappa^2 + \kappa_A^2(\mathbf{Q})]^{-1/2}, \quad (10)$$

depends now on $\mathbf{Q}$ direction determined by $\{\hat{Q}^4\} = \sin^4\vartheta(\cos^4\varphi + \sin^4\varphi) + \cos^4\vartheta$, where φ and ϑ are spherical angles in cubic coordinate frame with z axis along (0,0,1). As a result at $T=T_c$ we have $\xi = \sqrt{2B/|F|}(\infty, \sqrt{6}, \sqrt{3/2})$ for the $\langle 111 \rangle$, $\langle 110 \rangle$, and $\langle 001 \rangle$ directions, respectively.

The expression for the scattering cross section in Eq. (6) catches the main symmetry features of the problem, takes into account all interactions mentioned above, and explains qualitatively the previous data[10,11] as well as ones presented below. Remarkable features of Eq. (6) read as follows.

(i) For the unpolarized neutrons the scattering intensity is localized on a sphere with radius $Q=k$ and around the sharp maxima of the cubic diagonals.

(ii) For completely polarized neutrons ($P_0=1$) the scattering intensity depends on the angle ϕ between vectors $\mathbf{Q}$ and $\mathbf{P}_0$ as well as the sign of $D/|D|$, which determines the handedness of the chiral fluctuations: If $D/|D|>0$ and $D/|D|<0$ we have right-handed (clockwise) and left-handed (counterclockwise) fluctuations, respectively (cf. Ref. 21). For positive and negative signs the scattering intensity is maximal at $\mathbf{P}_0 \downarrow \uparrow \mathbf{Q}$ and $\mathbf{P}_0 \uparrow \uparrow \mathbf{Q}$, respectively. In both cases the intensity appears as half-rings. This pattern was observed in Ref. 10 and 11 and corresponds to the negative sign in agreement with the data in Ref. 21 obtained below T_c.

(iii) The AEI restores the conventional form of the critical fluctuations peaked along $\langle 111 \rangle$ (MnSi) or $\langle 001 \rangle$ (FeGe). However, their exact form and dependence on $\tau=(T-T_c)/T_c$ demands further theoretical and experimental work.

As a result we distinguish three (T,Q) regions:

(i) $Q \gtrsim \kappa(T) \gg k$, where the mean-field fluctuations have a conventional form and one can expect the ferromagnetic critical behavior (see for example Ref. 23).

(ii) In a rather narrow region $|Q-k| \gtrsim \kappa(T)$ and apart from the easy directions one can expect a crossover to quasi-one-dimensional critical behavior at $\kappa \sim k$.

(iii) There is strong anisotropy in $\mathbf{Q}$ space with three-dimensional critical regime along the easy directions $\langle 111 \rangle$ or $\langle 001 \rangle$ when $\Phi, \Theta < 1$.

One can expect that the critical dynamics in region (i) $(Q \gg \kappa \gg \kappa_A)$ are of ferromagnetic nature in agreement with results presented in Sec. IV. In region (ii) the critical slowing down has to be restricted first by the DMI at $\kappa \sim k$ showing the first crossover. The second crossover has to be in the easy directions near T_c and the critical slowing down can survive along the cubic diagonals only. It should be noted also that

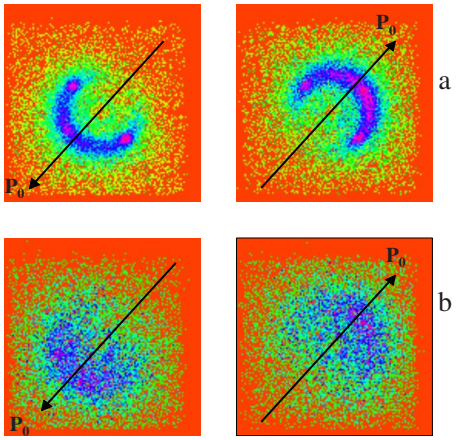

FIG. 2. (Color online) SANS maps of the critical scattering in MnSi at $\tau=(T-T_c)/T_c=0.007$ (a) and $\tau=0.042$ (b) for two opposite polarization directions $\mathbf{P}_0$.

our results obtained for the easy directions are in favor of a second-order transition.

It should be noted that the complex temperature behavior above T_c of the macroscopically measured quantities such as specific heat, conductivity, and the sound propagation[12,13] is in a qualitative agreement with the three region behavior discussed above. However, the mean-field theory presented above cannot give the correct values of the critical exponents for the susceptibility and correlation length, etc. The corresponding theoretical work has not been done yet except for the very first step in this direction done in Ref. 24, where strong renormalization of the chiral susceptibility was demonstrated. Nevertheless, we show that the mean-field theory presented above describes all experimental features of the thermal phase transition in MnSi at least on the qualititative level.

III. SMALL ANGLE POLARIZED NEUTRON SCATTERING

We have performed polarized SANS measurements on two single crystals of MnSi at the SANS-2 facility in Geesthacht (Germany). The two different samples, sample 1 and sample 2, the same as in Refs. 10 and 11, respectively, were used for the measurements. Two temperature scans of sample 1 and one scan of sample 2 were used to verify reproducibility of the results. The beam of polarized neutrons ($P_0=0.95$) was exploited at a wavelength $\lambda=0.58$ nm. The scattered neutrons were detected with a 2D position sensitive detector. The temperature stabilization was better than 0.05 K.

The scattering images for two different temperatures are given in Fig. 2. The diffuse scattering intensity just above T_c looks like half-moons oriented along the incident neutron polarization [Fig. 2(a)]. The sum of the intensities of two opposite polarizations form an anisotropic ring with weak spots, which below T_c transforms into the Bragg peaks, while the ring disappears. Upon increase in the temperature the half-moon shaped images are smeared [Fig. 2(b)]. The asymmetric P-dependent scattering is a fingerprint of the single spin chirality, so the DMI is responsible for the spiral ordering seems to be powerful enough in the whole critical range and has the single sign in the whole sample. This picture of scattering is in good agreement with the theory given in Sec. II and in Ref. 10.

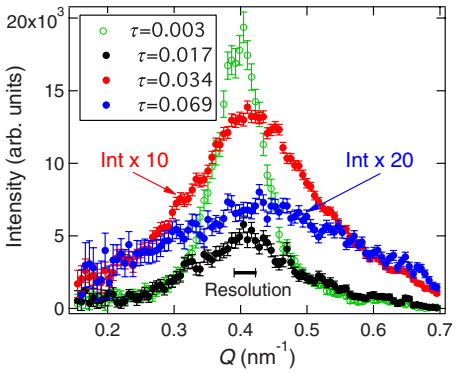

FIG. 3. (Color online) Momentum transfer dependence of the scattering intensity at different $\tau=(T-T_c)/T_c$ for $\mathbf{Q}\|[111]$. Two intensities are multiplied by factor 10 and 20 to highlight them on the graph.

The longitudinal q scan along the easy axes $\langle 111\rangle$ for different temperatures above T_c measured with unpolarized neutrons are shown in Fig. 3. These scans are well described by the Lorentzian of the form $C/[(Q-k)^2+\kappa^2]$ with the center at $Q=k\approx 0.4$ nm^{-1} for all the data taken above T_c. For the Bragg peaks taken below T_c these curves transform to Gaussian with the constant full width at half maximum (FWHM) (of order of 0.08 nm^{-1}) corresponding to the instrumental resolution. The critical temperature was experimentally found to be $T_c=28.80(7)$ K for sample 1 and $T_c=29.05(5)$ K for sample 2 as the point, where the transformation from Lorentzian shape to Gaussian shape occurs.

The Lorentzian parameters [the amplitude is proportional to the susceptibility at the Bragg point, $\chi(q=0)$ where $q=|Q-k|$, and FWHM proportional to the inverse correlation length $\xi^{-1}=\kappa$] were obtained from the fit. Their dependencies for three temperature scans are presented in Fig. 4 as a function of the reduced temperature in log-log scale.

The scaling laws of these two parameters exhibit a crossover at $\tau\approx 0.02$ where $\kappa\approx 0.75k$. The corresponding values are $\gamma_1=0.65(3)$ and $\nu_1=0.40(6)$ in the vicinity of T_c and $\gamma_2=1.61(2)$ and $\nu_2=0.68(1)$ for higher temperatures at $\kappa>0.75k$.

It is convenient sometimes to determine the so-called polarization of the scattering as

$$P_s(Q)=\frac{\sigma(\mathbf{P}_0)-\sigma(-\mathbf{P}_0)}{\sigma(\mathbf{P}_0)+\sigma(-\mathbf{P}_0)}=-\frac{2kQP_0\cos\phi}{Q^2+k^2+\kappa^2}, \qquad (11)$$

where ϕ is the angle between $\mathbf{P}_0$ and $\mathbf{Q}$ and we take Eq. (6) to estimate its value using parameters Q,k and κ. The temperature dependence of the polarization $P_s(Q=k)$ is shown in the inset of Fig. 4. As it is well seen and was also noted in Ref. 10 and 14, the polarization is close to 1 in the range 1–2 degrees above T_c, showing pure chiral fluctuating state within this range. This range is well correlated with the crossover behavior of $\chi(q=0)$ and κ. This pure chiral phase can be explained by the lock-in process occurring as soon as

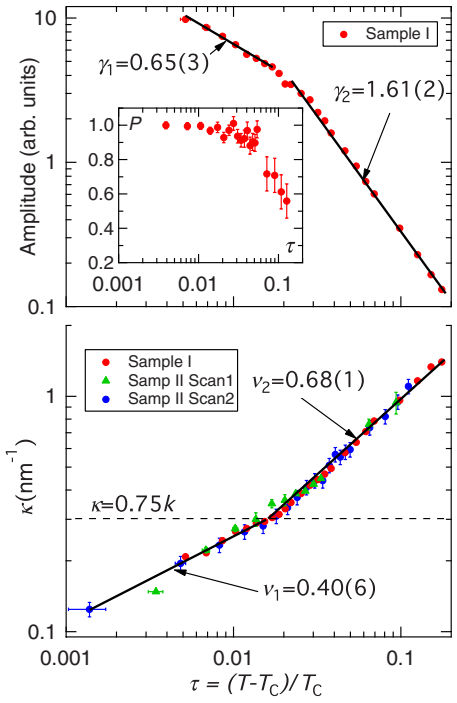

FIG. 4. (Color online) The Lorentzian amplitude and the inverse correlation length versus reduced temperature $\tau=(T-T_c)/T_c$ for $\mathbf{Q}\|[111]$. The inset shows the temperature dependence of polarization defined by Eq. (11).

κ becomes comparable with k. We would like to warn about the complex form of the correlation functions in MnSi [see Eq. (8)] and not trivial interpretation of the obtained numbers such as κ. Moreover, it must be noted that experimentally obtained value of κ shown in Fig. 4(b) is referred to the one in the denominator of Eq. (6), while the value of κ involved in Eq. (10) is referred to the one in the numerator of Eq. (6). Although this is the same value in the mean-field theory, these two values κ may be different from the experimental point of view. One can refer to Ref. 25, where the chiral and conventional parts of the susceptibility were extracted using the manipulations with the cross sections of the polarized neutrons as polarization dependent part and polarization independent part. The former is attributed to the pure chirality with the chiral susceptibility and the latter is attributed to the trivial nonchiral susceptibility. In our case this approach can shed an additional light onto the problem.

In this system the period of the helix structure $d=2\pi/k \approx 16$ nm is a scale where the isotropic exchange and DMI are of the same order.[10,15] The noncollinearity of the spin fluctuations is important close to the transition, where $2\pi\xi \geq d$. It reveals itself through the well-resolved half-moons in Fig. 2(a). On the other hand, if q or $\kappa \gg k$ this noncollinearity is inessential what leads to smearing of half-moons (Fig. 2(b)). In this case the nature of the fluctuations has to be the same as in conventional ferromagnets. Indeed, in high T region we have the exponent $\nu \simeq 2/3$ like in ferromagnets (see also detailed discussion in Sec. II).

It is worthwhile to note that the critical exponent of the order parameter $\beta=0.22(1)$.[10] Moreover, the same values of the critical exponents have been found for the relative systems. Particularly, $\beta=0.22(1)$ and $\nu=0.48(5)$ found in $Fe_{0.85}Co_{0.15}Si$,[26] suggest that these critical indexes are universal for the cubic magnets with the DMI. The scaling relation between the indexes $\gamma+2\beta=3\nu$ is well satisfied within the error bars for both temperature regions, i.e., close to T_c for the helixlike region and for the ferromagnetic like one, i.e., well above T_c. It may be considered as an evidence of the second-order transition summoned by small critical $\mathbf{Q}$ regions around easy $\langle 111 \rangle$ directions.

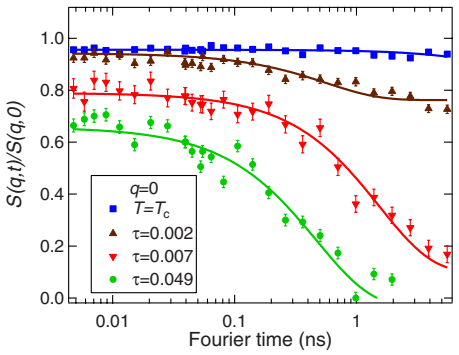

FIG. 5. (Color online) The temperature evolution in the critical region of the intermediate scattering function $S(q,t)$, $\mathbf{Q}\|[111]$, $q=|Q-k|=0$. Spectra were collected at $Q=0.4$ nm^{-1} with NSE spectrometer IN11 at ILL for $T=T_c$ (blue squares), $\tau=0.002$ (brown up triangles), $\tau=0.007$ (red down triangles), $\tau=0.049$ (green circles) respectively. The solid lines are the best fits to the data by simple exponential decay (12).

IV. NEUTRON SPIN ECHO

We have used the paramagnetic NSE technique to study the critical dynamics in MnSi.[27] The experiments were performed on the spin echo spectrometer IN11 at ILL, Grenoble (France) at the incoming neutrons wavelength $\lambda_0=0.65$ nm and for Q values $0.2 \div 0.6$ nm^{-1}. The results were supplemented by measurements at the wide angle NSE spectrometer SPAN at Helmholtz Zentrum für Materialen und Energie, Berlin (Germany) at $\lambda_0=0.45$ and 0.65 nm in the same Q range. The temperature stabilization accuracy was $\Delta T=0.01$ K. All NSE spectra were normalized by the resolution function of the spectrometers, determined at $T=2$ K well below T_c, where there is no inelastic contribution to the spin-echo signal visible by this technique. It is worthwhile to point out that the quasielastic part of the spectrum observed by the spin echo is seen just above of T_c only. The elastic signal dominates below T_c and inelasticity increases strongly with growing T. The measurements were performed with $\mathbf{Q}$ along two directions in the reciprocal space: [111] and [110].

The temperature evolution of the normalized intermediate scattering function $S(q,t)$ is shown for $\mathbf{Q}\|[111]$ $(q=0)$ in Fig. 5. A similar data set for $\tau=0.007$ and for different q values is shown in Fig. 6. The spectra span a dynamic range of three orders of magnitude and the dynamics of the helical fluctuations lie within the NSE window.

The data were fitted using the exponential decay

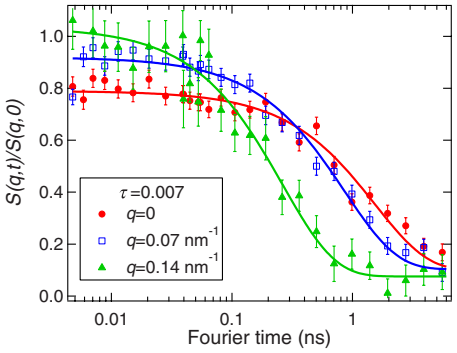

FIG. 6. (Color online) The intermediate scattering function $S(q,t)$, $\mathbf{Q}\|[111]$ at $\tau=0.007$ for different reduced momentum transfer values: $q=0$ (closed red circles), $q=0.07$ nm^{-1} (open blue squares), $q=0.14$ nm^{-1} (closed green triangles), respectively. The solid lines are the best fits to the data by simple exponential decay (12).

$$S(q,t) = y_0 + A\ \exp\left(-\frac{t}{\tau_0}\right), \tag{12}$$

where τ_0 is the relaxation time of the critical fluctuations, y_0 is the elastic background, and A is the scaling factor. The solid lines are the best least square fits to the data of an exponential decay (12). The background value y_0 is negligible for the entire temperature range, when $\mathbf{Q}\|[111]$ or $q \neq 0$, i.e., far enough from the Bragg point. However, y_0 significantly increases when the temperature decrease for $\mathbf{Q}\|[111]$ orientation and small q values, i.e., close to the Bragg point. Apparently it can be associated with the first-order transition,[12] when the elastic contamination to the signal occurs in the close vicinity of T_c. The relaxation rate was obtained from these fits using the relation $\Gamma[\mu\text{eV}] = 1.317/\tau_0[\text{ns}]$.[28]

The momentum transfer dependence of the relaxation rate Γ is plotted in Fig. 7 for $T=29$, 31, and 33 K. It is important to note that one has to use the reduced momentum transfer

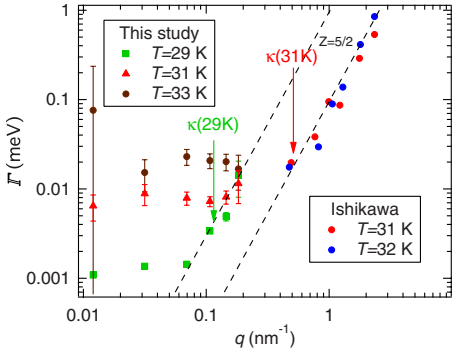

FIG. 7. (Color online) The log-log plot of the momentum transfer dependence of the relaxation rate Γ for $\mathbf{Q}\|[111]$ at different temperatures $T=29$ K (green squares), 31 K (red triangles), and 33 K (brown circles). These data are combined with those available from the literature (Ref. 29) (red and blue circles). The closed red symbols from two different sources (triangles—this study, circles—Ishikawa) show the data taken at the same temperature $T=31$ K. The black dashed lines represent the 5/2 scaling law.

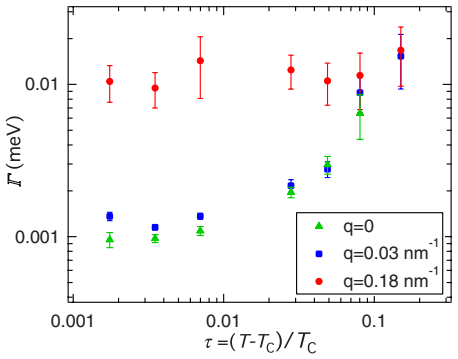

FIG. 8. (Color online) The log-log plot of the temperature dependence of the relaxation rate Γ for small $q=0$, $q=0.03$ nm^{-1} and large $q=0.18$ nm^{-1}.

$\mathbf{q}=\mathbf{Q}-\mathbf{k}$. The obtained values of Γ are combined with those available from the paper of Ishikawa.[29] The data at $T=29$ K (squares) saturates at small q and follow $q^{5/2}$ scaling law at $q \geq 0.07$ nm^{-1}. The triangles representing our data at $T=31$ K, in combination with the data from Ref. 29, show the similar behavior. Hence, both data sets: squares at $T=29$ K and symbols at $T=31$ K have a tendency to approach black dashed lines (see Fig. 7), representing the dynamic scaling law $\Gamma \sim q^{5/2}$ for large q values similar to that in ferromagnets.[23] As it is also expected from the dynamical scaling theory, Γ has to saturate in the range $q<\kappa$ due to violation the total spin conservation law by the DMI. The values of κ for $T=29$ and 31 K are pointed by arrows in Fig. 7. Hence it is not surprising that for $T=33$ K, Γ does not change within the range of the measured momentum transfer $q<0.2$ nm^{-1}. This shows that the correlation length $\xi=\kappa^{-1}$ is an effective parameter in the dynamics of the fluctuations limiting the lowest energy by the value of $\Gamma(\kappa)$ similar to those observed in Fe (see for example, Fig. 2 in Ref. 27).

The temperature dependences of the relaxation rate Γ for different q smaller than κ and $q \geq \kappa$ are shown in Fig. 8. For the large q (circles) the value of Γ does not change with the temperature demonstrating that it depends solely on q. For the small q it seems to be determined by the value of κ and becomes independent of T at very small τ where $q>\kappa, (\tau<0.017)$.

In spite of obvious lack of the experimental points to determine a law for the temperature change in Γ we took a risk to fit the data at small q and at large temperatures ($\tau>0.017$) to the power law $\Gamma \sim \tau^{Z\nu}$, that gives the value of $Z\nu \simeq 1.8(2)$. To better see the relation between $\Gamma(q=0)$ and κ we plot the one versus another in the log-log scale in Fig. 9. The dependence of line width, Γ, on the inverse correlation length, κ, exhibits the scaling law $\Gamma=A\kappa^Z$ with the crossover from (i) $Z=2.49(9)$ for large κ (large T) to (ii) $Z=1.10(4)$ for small κ (close to T_c). It holds approximately at the same τ as the crossover in κ and χ behavior (Fig. 3). Finally, we conclude that the relaxation rate changes strongly with temperature at $\tau>0.025$ obeying the scaling law with $\Gamma(q=0) \sim \kappa^{Z_2} \sim \tau^{Z_2\nu_2}$ with $Z_2=2.5(1)$ and $\nu_2=0.69(3)$. Then $\Gamma(q=0)$ has a crossover to the regime at $\tau<0.025$ obeying a scaling law with $\Gamma(q=0) \sim \kappa^{Z_1} \sim \tau^{Z_1\nu_1}$ with $Z_1=1.10(4)$ and $\nu_1=0.38(5)$.

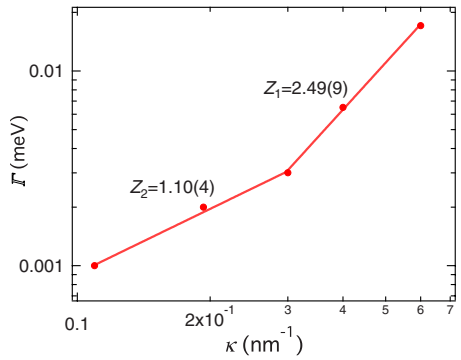

FIG. 9. (Color online) The log-log plot of the relaxation rate $\Gamma(q=0)$ versus the corresponding inverse correlation length, κ, taken through the whole critical temperatures. Solid lines are the best least square fit with power law.

The critical dynamics of MnSi had been studied using triple axis neutron spectrometry by Ishikawa *et al.*,[6,29] where the magnetic system of MnSi was considered as an example of the weak itinerant ferromagnet. Contrary to the predictions of the dynamic scaling theory confirmed experimentally for itinerant Fe, Co, and Ni as well as dielectric EuO and EuS (see Ref. 23 and references therein) giving the critical fluctuation's line width by

$$\Gamma = A_0 q^{5/2} f(\kappa/q), \tag{13}$$

the authors in Ref. 29 interpreted the obtained data in terms of the itinerant magnet theory with the line width given by[29]

$$\Gamma = A_1 q(q^2 + \kappa^2). \tag{14}$$

Both theories [Eqs. (13) and (14)] give very similar values for the line width in the large q range ($q \gg \kappa$) proportional to $q^{5/2}$ and q^3, respectively. Therefore, the Γ values obtained at large q region could fit to both theories. The significant difference occurs in the small q range ($q \ll \kappa$). Here for the itinerant model the line width depends linearly on q. In the dynamical scaling theory it is proportional to $q^2\kappa^{1/2}$, due to the total spin conservation requirements in the exchange approximation.

However, both theories hold for the ferromagnets when $\mathbf{q}=\mathbf{Q}$, but not for helimagnets, when $\mathbf{q}=\mathbf{Q}-\mathbf{k}$. Therefore, they can be applied to $P2_13$ helimagnets only in the large-q region, where $q \gg k$ and the DMI may be neglected. At present there is no theory of the critical dynamics of the $P2_13$ magnets for the range $q \leq k$. Our experimental data taken for small-q range show no q dependence of Γ at $q < \kappa$ and Γ depends only on q at $q > \kappa$ as $\Gamma \sim q^{5/2}$. The former may be explained by the violation of the total spin conservation low due to presence of DMI. The latter well corresponds to the ferromagnetic scaling behavior[23] as soon as the DMI is neglected. At $q \leq \kappa(T) \leq k$ a scaling behavior should be expected, where $\Gamma \sim \kappa$, both change slowly with temperature.

V. CONCLUSIONS AND REMARKS

We report on the crossover in the critical behavior in MnSi from high T ferromagnetic like fluctuations to the close to T_c helixlike regime. The crossover is associated with an influence of the DMI, responsible for the chiral ordering: it dominates close to T_c and weakens for higher temperatures.

(i) We present the essence of a theory describing the polarized neutron critical scattering in the helimagnet MnSi and similar compounds. The theory is based on the hierarchical Bak-Jensen model of the three interactions (FE, DMI, and AEI) and it predicts the appearance of three ranges in the critical scattering. A ferromagnetic like regime occurs in the high-T limit, where DMI and AEI may be neglected. The intermediate region, where the DMI becomes important, is characterized by critical fluctuations localized on the spherical surface at $Q=k$. The crossover in the susceptibility $\chi(r)$ between these two regions is examined. It was demonstrated that the critical fluctuations in the second region have a very unusual form. Close to the transition the anisotropic exchange interaction restores conventional three-dimensional form of the critical fluctuations in rather narrow regions near easy $\langle 111 \rangle$ directions, where the magnetic Bragg peaks appear below the transition.

(ii) The inverse correlation length κ and the susceptibility χ were measured in the easy direction using polarized neutron scattering (SANS). The temperature dependences of both quantities demonstrate the crossover at $\tau \approx 0.02$ where $\kappa \sim k$. In the vicinity of T_c the critical exponents of the susceptibility χ and κ are equal $\gamma_1=0.65(3)$ and $\nu_1=0.40(6)$, respectively, whereas at higher T ($\kappa > k$), $\gamma_2=1.61(2)$ and $\nu_2=0.68(1)$. We argue that the crossover, revealed in the change in indexes for κ and χ at $\kappa \sim k$, is compatible with the theory mentioned above: the short-range correlations reveal their ferromagnetic like nature, while the long-range correlations along the easy directions have the helixlike nature with strong influence of both DMI and AEI.

(iii) The relaxation rate Γ of the critical fluctuations along the easy direction was measured in the range of small $\mathbf{q}=\mathbf{Q}-\mathbf{k}$. This q region is easily accessible for the NSE technique and difficult for the triple axis spectroscopy due to the resolution restrictions. It is also shown that the critical dynamics are compatible with the general form of the dynamical scaling theory Eq. (13) and undergoes a crossover from a high-temperature ferromagnetic like regime with the critical exponent $Z_2=2.5(1)$ to a helixlike regime with $Z_1=1.10(4)$ close to T_c. The applicability of the dynamical scaling theory for $q \gg \kappa$ is not surprising accounting for the ferromagnetic nature of the fluctuations at relatively high temperatures. We argue that the form of the dynamical scaling, which appears very close to T_c where $\kappa \ll k$, is determined by the DMI and AEI. We point out that the dynamical and static crossovers to behavior are best pronounced along the easy $\langle 111 \rangle$ directions only. In other directions the critical fluctuations demonstrate behavior compatible with a first-order transition to the long-range helical state.

(iv) We belive that the mean-field theory and the neutron cross section calculated on its basis [Eq. (6)] explains at least qualitatively existing experimental neutron scattering data for MnSi.[3,10,11] We insist that our theory is the real alternative to the skyrmion assumption that was proposed in Ref. 17 and used in Ref. 14 to explain the experimental results close to T_c. To our opinion the use of the skirmionic assumpsion is especially counterproductive in view that the authors of Ref.

17 gave no detailed predictions or evaluations for susceptibility and the neutron cross section.

ACKNOWLEDGMENTS

We acknowledge C. Pappas for the help in spin-echo measurements and fruitful discussions. The PNPI team acknowledges GKSS and HZB for hospitality. The Russian authors thank for partial support the Russian Foundation of Basic Research (Grants No. 09-02-00229, No. 09-02-01023, and No. 10-02-01205) and Russian State programs "Neutron research in solids," "Strongly correlated electrons in semiconductors, metals, superconductors, and magnetic materials," and "Quantum macrophysics."

*grigor@pnpi.spb.ru

[1] C. Pfleiderer, G. J. McMullan, S. R. Julian, and G. G. Lonzarich, Phys. Rev. B **55**, 8330 (1997).
[2] S. R. Julian and G. G. Lonzarich, Nature (London) **414**, 427 (2001).
[3] C. Pfleiderer, D. Reznik, L. Pintschovius, H. v. Löhneysen, M. Garst, and A. Rosch, Nature (London) **427**, 227 (2004).
[4] P. Pedrazzini *et al.*, Phys. Rev. Lett. **98**, 047204 (2007).
[5] Y. Ishikawa, K. Tajima, D. Bloch, and M. Roth, Solid State Commun. **19**, 525 (1976).
[6] Y. Ishikawa, G. Shirane, J. A. Tarvin, and M. Kohgi, Phys. Rev. B **16**, 4956 (1977).
[7] G. Shirane, R. Cowley, C. Majkrzak, J. B. Sokoloff, B. Pagonis, C. H. Perry, and Y. Ishikawa, Phys. Rev. B **28**, 6251 (1983).
[8] S. V. Grigoriev, D. Chernyshov, V. A. Dyadkin, V. Dmitriev, S. V. Maleyev, E. V. Moskvin, D. Menzel, J. Schoenes, and H. Eckerlebe, Phys. Rev. Lett. **102**, 037204 (2009).
[9] B. Roessli, P. Böni, W. E. Fischer, and Y. Endoh, Phys. Rev. Lett. **88**, 237204 (2002).
[10] S. V. Grigoriev, S. V. Maleyev, A. I. Okorokov, Y. O. Chetverikov, R. Georgii, P. Boni, D. Lamago, H. Eckerlebe, and K. Pranzas, Phys. Rev. B **72**, 134420 (2005).
[11] S. V. Grigoriev, S. V. Maleyev, A. I. Okorokov, Y. O. Chetverikov, P. Boni, R. Georgii, D. Lamago, H. Eckerlebe, and K. Pranzas, Phys. Rev. B **74**, 214414 (2006).
[12] S. M. Stishov, A. E. Petrova, S. Khasanov, G. K. Panova, A. A. Shikov, J. C. Lashley, D. Wu, and T. A. Lograsso, Phys. Rev. B **76**, 052405 (2007).
[13] S. M. Stishov, A. E. Petrova, S. Khasanov, G. K. Panova, A. A. Shikov, J. C. Lashley, D. Wu, and T. A. Lograsso, J. Phys.: Condens. Matter **20**, 235222 (2008).
[14] C. Pappas, E. Lelièvre-Berna, P. Falus, P. M. Bentley, E. Moskvin, S. Grigoriev, P. Fouquet, and B. Farago, Phys. Rev. Lett. **102**, 197202 (2009).
[15] P. Bak and M. H. Jensen, J. Phys. C **13**, L881 (1980).
[16] I. E. Dzyaloshinskii, Zh. Eksp. Teor. Fiz. **46**, 1420 (1964).
[17] U. K. Rössler, A. N. Bogdanov, and C. Pfleiderer, Nature (London) **442**, 797 (2006).
[18] S. Mühlbauer, B. Binz, F. Jonietz, C. Pfleiderer, A. Rosch, A. Neubauer, R. Georgii, and P. Böni, Science **323**, 915 (2009).
[19] S. V. Maleyev, Phys. Rev. B **73**, 174402 (2006).
[20] M. Tanaka, H. Takayoshi, M. Ishida, and Y. Endoh, J. Phys. Soc. Jpn. **54**, 2970 (1985).
[21] M. Ishida, Y. Endoh, S. Mitsuda, Y. Ishikawa, and M. Tanaka, J. Phys. Soc. Jpn. **54**, 2975 (1985).
[22] S. V. Maleyev, J. Phys.: Condens. Matter **21**, 146001 (2009).
[23] O. W. Dietrich, J. Als-Nielsen, and L. Passell, Phys. Rev. B **14**, 4923 (1976).
[24] S. Tewari, D. Belitz, and T. R. Kirkpatrick, Phys. Rev. Lett. **96**, 047207 (2006).
[25] V. P. Plakhty, W. Schweika, T. Brückel, J. Kulda, S. V. Gavrilov, L.-P. Regnault, and D. Visser, Phys. Rev. B **64**, 100402(R) (2001).
[26] V. A. Dyadkin, S. V. Grigoriev, E. V. Moskvin, S. V. Maleyev, D. Menzel, J. Schoenes, and H. Eckerlebe, Physica B **404**, 2520 (2009).
[27] F. Mezei, Phys. Rev. Lett. **49**, 1096 (1982).
[28] F. Mezei, C. Pappas, and T. Gutberlet, *Neutron Spin Echo Spectroscopy*, Lecture Notes in Physics Vol. 601, (Springer-Verlag, New York, 2003).
[29] Y. Ishikawa, Y. Noda, Y. J. Uemura, C. F. Majkrzak, and G. Shirane, Phys. Rev. B **31**, 5884 (1985).